



Extended summary

Dynamic Behaviour of Deep Foundations with Inclined Piles

Curriculum: Materials, Water and Soil Engineering

Author

Michele Morici

Tutors

Prof. Ing. Giuseppe Scarpelli

Ing. PhD Fabrizio Gara

Date: 30- January-2014

Abstract. The paper presents a numerical model for the kinematic interaction analysis of inclined pile groups; piles are modelled with beam finite elements and the soil is schematized with independent horizontal infinite layers. The pile-soil-pile interaction and the radiation problem are accounted by means of elastodynamic Green's functions. Piles cap is considered by introducing a rigid constraint; the condensation of the problem permits a consistent and straightforward derivation of both the impedance functions and the foundation input motions which are necessary to perform the inertial soil-structure interaction analyses, according to the substructure approach. The model, which also allows evaluating the kinematic stress resultants in piles resulting from the propagation of seismic waves in the soil, is validated performing accuracy analyses and comparing results, in terms of dynamic impedance functions, kinematic response parameters and pile stress resultants, with those furnished by 3D refined finite element models. Finally, a case study is presented to exhibit the capability of the proposed model to capture the effects of pile inclination on the superstructure and foundation response.

Keywords. Finite Element Model, Impedance Functions, Inclined Piles, Kinematic Interaction Analysis, Pile Kinematic Stress Resultants.

1 Introduction

Inclined piles are naturally able to resist higher lateral loads than vertical ones having the same diameter and length, as part of the force is axially transmitted. Piles are thus less stressed by shear and bending, with the advantage of limiting the pile diameter, especially in the case of soft soils. However, as a consequence of their poor performance in past earthquakes, the use of inclined piles in seismic areas is not recommended by modern codes [1, 2]. Among others, some examples of such negative performances are the wharfs of the Port of Oakland, during the 1989 Loma Prieta Earthquake, and the Port of Los Angeles, during the 1994 Northridge Earthquake.

Investigations on the causes of failures in past earthquakes demonstrated that in many cases the poor connection at the cap or the inappropriate pile design have determined the observed damages [3]. Indeed, inclined piles may induce large forces on the pile cap and permanent rotations may arise during strong earthquakes; furthermore, piles bending moment capacity may be reduced by the high axial force. These aspects should be carefully taken into account in the design to guarantee a good seismic performance of inclined pile groups. Evaluation of actual causes of failures, in conjunction with the advantages that may derive from a proper design, are the main reasons why the use of inclined piles is nowadays increasing again. Consequently, many works have been published recently on this topic, among the others, the papers of Sadek and Shahrour [4], Gerolymos et al. [5], Giannakou et al. [6] and Padrón et al. [7] are herein quoted.

In this paper a numerical model for the kinematic interaction analysis of inclined pile groups is presented, by generalizing the procedure proposed by Dezi et al. [8] for vertical piles. Piles are modelled with beam finite elements and the soil is assumed to be a horizontally layered half-space. Both piles and soil behave linearly and the pile-soil-pile interaction and the radiation damping are taken into account in the frequency domain by means of elastodynamic Green's functions. The presence of a rigid cap is accounted for by constraining the displacements of the pile heads. The model allows evaluating the kinematic response of pile groups with generic number of piles, generic layout and piles inclination; in particular the motion of the pile cap and the stress resultants in piles due to the passage of harmonic shear or seismic waves in the soil may be computed; in the latter case, the incoming free field may be derived from local one dimensional or spatial analysis depending on the complexity of the site. Furthermore, the condensation of the problem on the rigid cap *dofs* allows obtaining impedances of the pile group; these may be used, in conjunction with the pile cap motion, to perform consistent soil-structure interaction analyses according to the substructure approach. The model is validated comparing results with those available in the literature or obtained from 3D refined finite element models. The model revealed to be efficient and able to capture without significant loss of accuracy the soil-foundation dynamic behaviour predicted by more rigorous models (e.g. boundary element formulations) or more sophisticated finite element models. Furthermore, the saving in terms computational time is very high as compared with 3D refined finite element model and may be significant even in the case of boundary element base approaches, especially in the case of stratified media. Finally, a case study is presented to exhibit the capability of the proposed model to capture the effects of pile inclination on the superstructure and foundation response. Bridge piers constituted by single columns and founded on inclined pile groups characterised by different configurations are considered. Real accelerograms are selected

with reference to rock outcropping (soil type A) and iteratively propagated by means of a 1D site response analysis and scaled to achieve at the deposit surface the design spectral acceleration at the fundamental period of the bridge (evaluated at fixed base condition). In this way amplifications of the specific site are accounted for by maintaining the compatibility at the ground surface with the code spectrum. The nonlinear soil behaviour is accounted for in a linear equivalent manner. Effects of the foundation layout on the superstructure and foundation dynamic response are illustrated.

2 Proposed Model

A numerical model for the kinematic interaction analysis of inclined pile groups is presented, by generalizing the procedure proposed by Dezi et al. [8] for vertical piles. The group may be constituted by a generic number of piles each of one may be characterised by a different rake angle; for the sake of simplicity, the projection of the pile length on the vertical direction is assumed to be the same for all the piles (Figure 1a).

Beam elements are used to model the piles that are embedded in a horizontally layered soil profile schematised by independent horizontal infinite layers (Baranov's assumption). Both piles and soil behave linearly and the problem is formulated in the frequency domain. The pile-soil-pile interaction and the radiation damping are taken into account by means of elastodynamic Green's functions. The problem solution is achieved with the finite element method (Figure 1b).

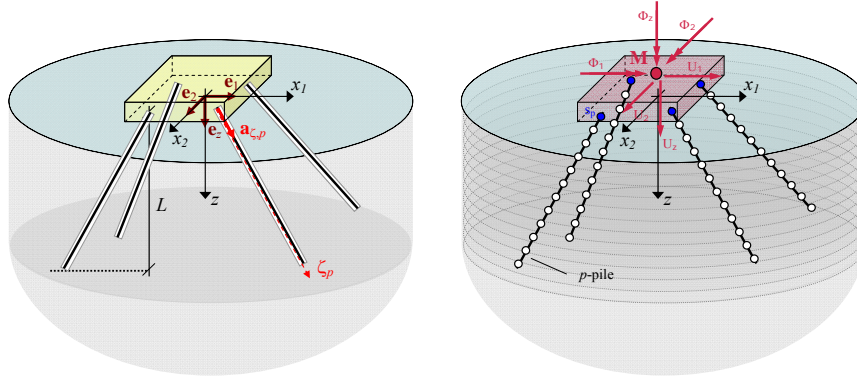


Figure 1. (a) Pile group with inclined piles and (b) proposed model.

The presence of a rigid cap is accounted for by defining a master node and introducing a rigid constraint at the pile heads; the problem condensation allows obtaining the impedance matrix \mathfrak{I} of the pile group. Depending on the pile group layout the master node degrees of freedom may be coupled and matrix \mathfrak{I} is generically fully populated. For layouts characterised by a double symmetry, by suitably positioning the master node at the intersection of the symmetry axes, the impedance matrix \mathfrak{I} assumes the form

$$\mathfrak{I}(a_0) = \begin{bmatrix} \mathfrak{I}_{x_1} & 0 & 0 & 0 & \mathfrak{I}_{x_1-rx_2} & 0 \\ & \mathfrak{I}_{x_2} & 0 & -\mathfrak{I}_{x_2-rx_1} & 0 & 0 \\ & & \mathfrak{I}_z & 0 & 0 & 0 \\ & & & \mathfrak{I}_{rx_1} & 0 & 0 \\ sym & & & & \mathfrak{I}_{rx_2} & 0 \\ & & & & & \mathfrak{I}_{rz} \end{bmatrix} \quad (1)$$

3.1 Numerical convergence

Accuracy analyses are performed with reference to H# and TL#, by varying the pile rake angle θ and taking into account different finite element length-pile diameter ratios ($L_e/d = 5; 3; 1; 0.5$). For the sake of brevity only some results will be shown. Figure 3a reports, for $\theta = 20^\circ$, for different E_p/E_s ratios and configuration H#, the non-dimensional stiffness and damping coefficients of the translational impedances obtained for all the L_e/d ratios. Figure 3b shows for configuration H1, the pile cap displacements obtained from steady analyses in which harmonic shear waves are propagated from the bedrock; the horizontal cap displacement U_M is normalised with respect to the amplitude of waves at the bedrock U_b while the cap rotation Φ_M is normalised with respect to the ratio between the pile diameter and the amplitude of waves at the bedrock. For the sake of brevity only results relevant to C1 with pile-soil modulus ratio $E_p/E_s = 1000$ and pile rake angle $\theta = 20^\circ$ are reported in this case. Finally, Figure 4 shows the normalized absolute values of kinematic stress resultants in one pile of H2 due to steady propagating shear waves with frequencies close to the first fundamental frequency of the soil deposit. In particular, results relevant to pile-soil modulus ratio $E_p/E_s = 1000$ and pile rake angle $\theta = 20^\circ$ are herein shown.

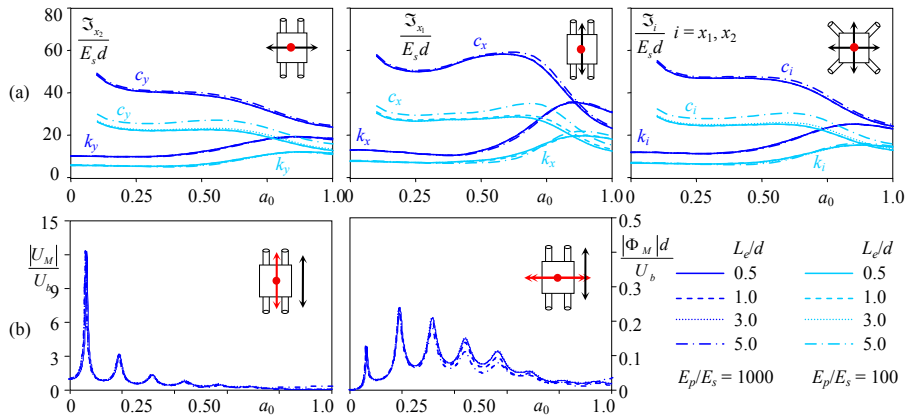


Figure 3. (a) Translational impedances of H1 and H2 for $\theta = 20^\circ$ and different pile-soil modulus ratios, by varying the L_e/d ratio; (b) displacements of pile cap of H1 for $\theta = 20^\circ$ and $E_p/E_s = 1000$, by varying the L_e/d ratio

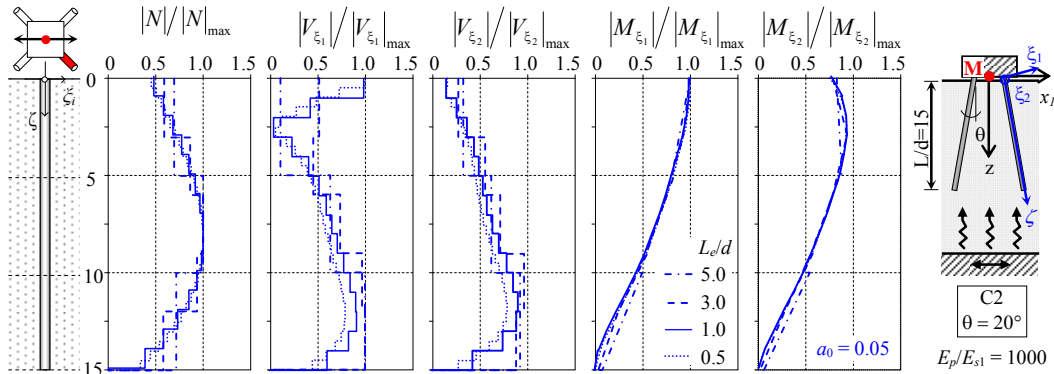


Figure 4. Kinematic stress resultants in one pile of H2, for $\theta = 20^\circ$ and $E_p/E_s = 1000$, by varying the L_e/d ratio

In the investigated frequency range convergence of impedances, as well as of displacements and stress resultants in piles, is very fast and even coarse meshes guarantee a good accuracy. For the subsequent analyses $L_e/d = 1$ is assumed.

3.2 Comparisons with 3D solid model

Results provided by the proposed model are compared with those obtained from refined 3D finite element analyses (Figure 5a) performed with the computer software ABAQUS. 8-node linear brick elements are used to model a cylindrical soil portion with diameter D and height T satisfying condition $D/d = 50$ and $T/d = 25$. The built-in frequency domain viscoelastic material model is adopted for the soil. Infinite elements are provided at the boundaries to absorb the outgoing waves and satisfy the radiation condition. Piles are modelled with 2-node cubic beam elements but their physical dimensions are taken into account by removing the relevant cylinders of soils. The beam solid coupling is assured exploiting potentials of the adopted software; furthermore, piles are connected at the head by a rigid constraint (Figure 5b). Meshing criteria aim at obtaining an as much as possible structured mesh and assuring a sufficient number of nodes per wavelength.

Some accuracy analyses are preliminarily performed to define the mesh dimension in order to balance reliability of results and the computational efforts; in particular, the mesh dimension is selected so as the propagation of waves with frequency up to $a_0 = 0.8$ are well captured. As for the proposed model, a finite element length-pile diameter ratio $L_e/d = 1$ is assumed, consistently with observations of previous section.

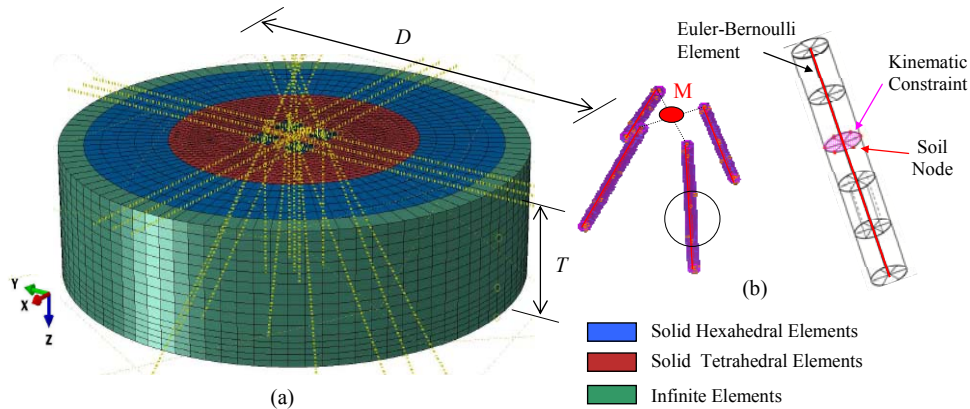


Figure 5. (a) 3D refined finite element model; (b) details of the kinematic constraint simulating the pile dimension and the rigid constraint simulating the pile cap

Figure 6 shows the non-dimensional stiffness and damping coefficients of the horizontal impedances of configurations H#, obtained by considering two pile-soil modulus ratios ($E_p/E_s = 100; 1000$) and two pile rake angles. Results obtained from the 3D refined finite element model are reported with symbols and the frequency range in which the solution may be inaccurate is highlighted in grey. These results are obtained by imposing unit steady-state harmonic displacements at the master node fully restrained, and evaluating the relevant reaction forces. Impedances are sensitive to the pile rake angle; the static lateral stiffness increases by increasing the rake angle as a consequence of the greater pile axial contribution to the response. (this is evident in the x_1 direction for configurations H1 and in both directions for configurations H2). On the other hand, as expected, for configura-

tions H1 in the x_2 direction the static stiffness is only slightly influenced by the pile inclination. With reference to stiff soils ($E_p/E_s = 100$), independently from the pile rake angle, the model is able to well capture both the static stiffness of the pile group and the frequency dependence of the stiffness coefficient, even if a slight frequency shift of the peak response is evident with respect to the results of the 3D solid model. On the other hand, for soft soils ($E_p/E_s = 1000$) greater inaccuracies are evident; the stiffness coefficient is overestimated at low frequencies (for a_0 up to 0.3) and underestimated at higher frequencies. Concerning damping coefficients, it can be observed that for stiff soils ($E_p/E_s = 100$) the model is able to reproduce with a good level of accuracy the benchmark results within the whole frequency range while for soft soils ($E_p/E_s = 1000$) the proposed model overestimate sensibly the damping coefficients at low frequencies (a_0 smaller than 0.2) and overestimates those at higher frequencies.

Figure 7 refers the non-dimensional stiffness and damping coefficients of the vertical impedance obtained from the same analysis cases. Even in this case the pile rake angle strongly affects the frequency dependence of impedances, as a consequence of the different contribution of flexural and axial pile behaviour. The model behaves very well as the stiffness and damping coefficients obtained from the refined 3D solid model are reproduced closely within the whole frequency range.

Figure 8 concerns rotational impedances; for both the H# configurations and for stiff and soft soils, stiffness coefficients obtained from the proposed model are close to those obtained from the refined 3D solid model. On the other hand, damping coefficients are characterised by some inaccuracies, especially at low frequencies.

Figure 9 refers to the coupled roto-translational soil-foundation behaviour; even in this case, the model behaves well and both stiffness and damping coefficients of the 3D solid model are captured with a sufficient level of accuracy within the whole frequency range for both the H# configurations.

Finally, Figure 10 reports the stiffness and damping coefficients of the torsional impedance of the selected case studies; the model is able to reproduce well the stiffness coefficients of both pile group configurations while damping coefficients are generally underestimated.

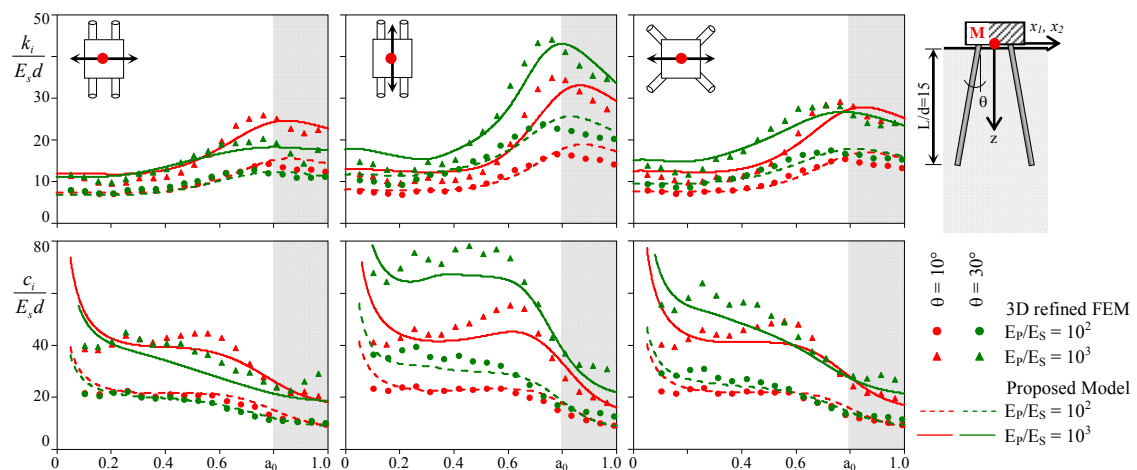


Figure 6. Lateral dynamic impedances for configuration H#, for two E_p/E_s ratios and two pile rake angles

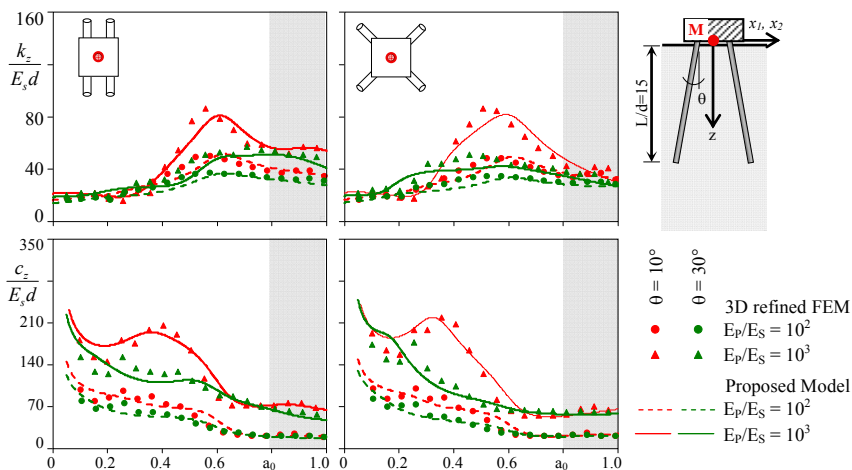


Figure 7. Vertical dynamic impedances for configuration H#, for two E_p/E_s ratios and two pile rake angle.

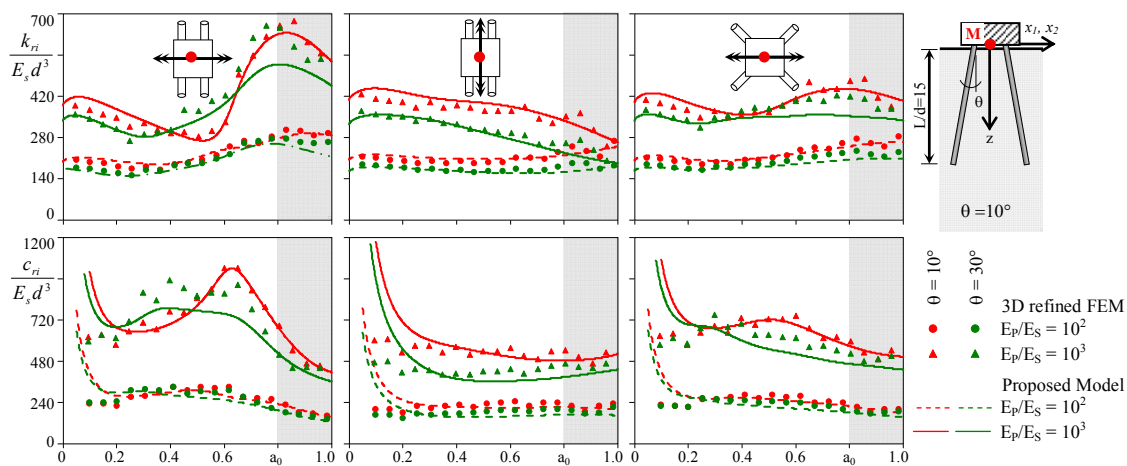


Figure 8. Rotational dynamic impedances for configuration H#, for two E_p/E_s ratios and two pile rake angles.

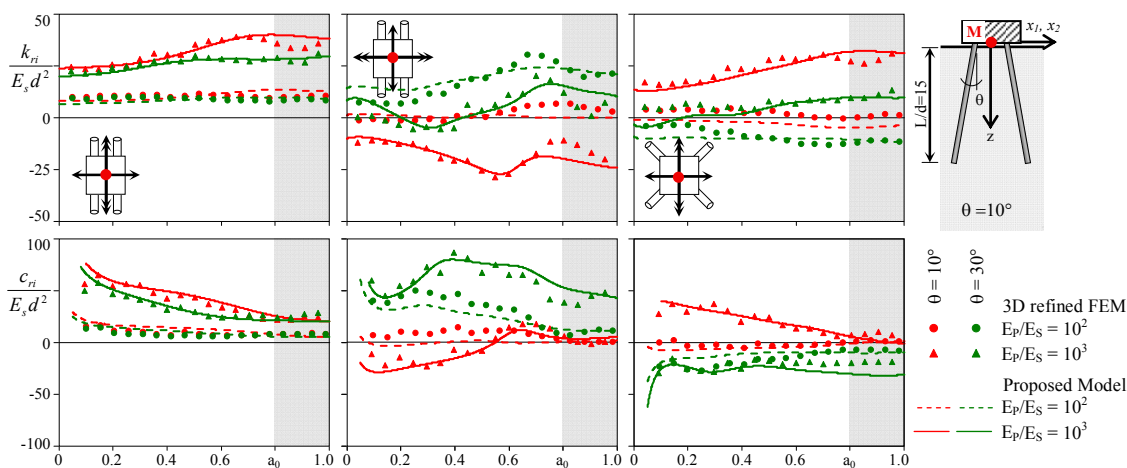


Figure 9. Roto-translational dynamic impedances for configuration H#, for two E_p/E_s ratios and two pile rake angles.

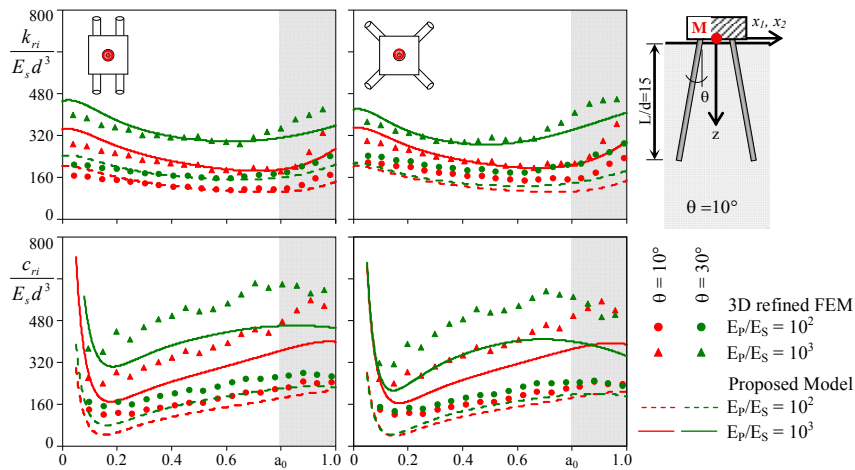


Figure 10. Torsional dynamic impedances for configuration H#, for two E_p/E_s ratios and two pile rake angles.

Figure 11 shows displacements of the pile cap obtained from steady analyses in which harmonic shear waves are propagated from the bedrock. Results obtained by considering pile group configurations H#, different pile-soil modulus ratios ($E_p/E_s = 100; 1000$) and pile rake angles are presented; the solution of the proposed model is reported with continuous and dashed lines while results of the 3D refined solid model are plotted with dots. It can be observed that, by increasing the pile rake angle the translational response of the group slightly decreases while the rotational response increases sensibly; in particular, amplitudes of peaks resulting from a rake angle of 30° are almost twice those obtained for vertical piles. In any case, the model is able to capture very well the kinematic response of the soil-pile group system, obtained from the refined 3D solid model.

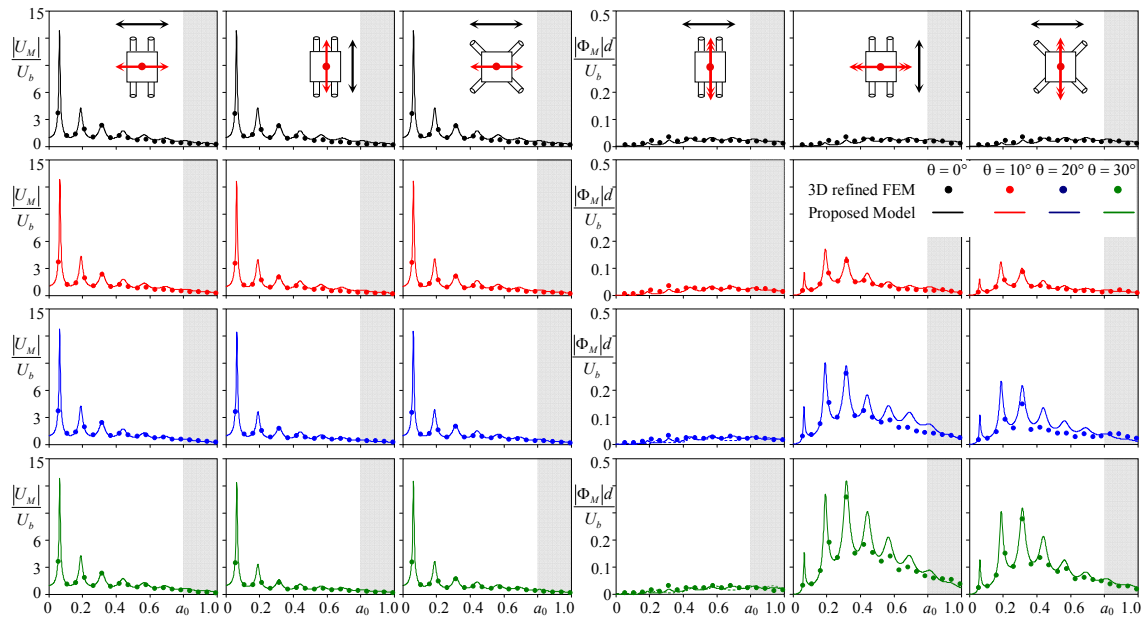


Figure 11. Kinematic response of pile cap for configuration H# and for two $E_p/E_s = 100$.

Figure 12 and shows the absolute values of the kinematic stress resultants in one pile of the group of the configuration H2 due to steady propagating shear waves with frequencies close to the first and second fundamental frequencies of the soil deposit (reported in the

figure). Axial force, shear forces and bending moments, normalised with respect to the maximum values attained within the pile shaft, are compared with the relevant values resulting from the 3D refined solid model. The model behaves very well since all the kinematic stress resultants estimated with the 3D solid model are reproduced closely.

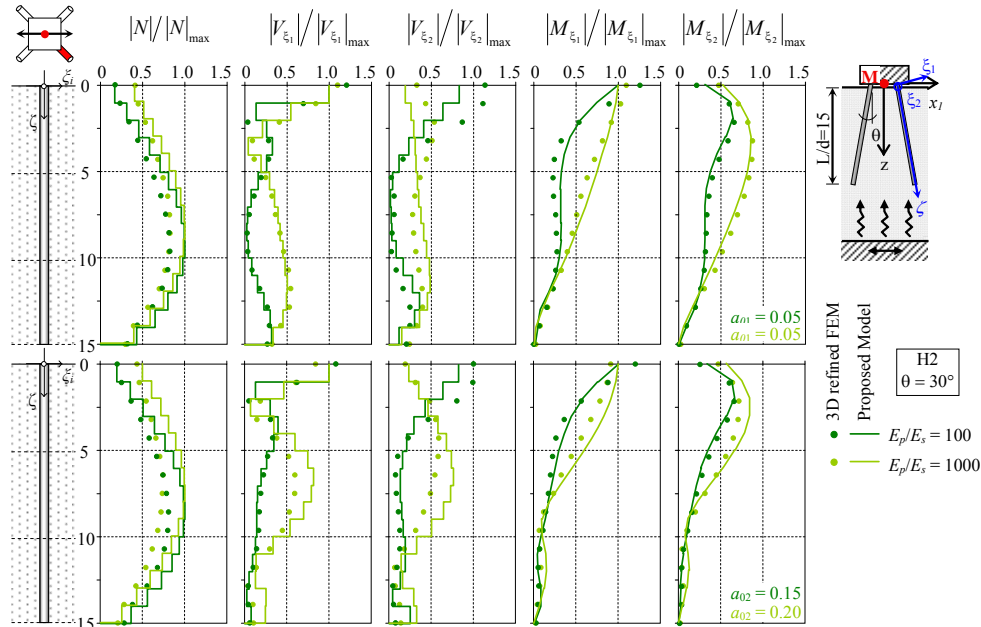


Figure 12. Kinematic stress resultants along one pile of the H2 configuration, for two pile rake angles and two different pile-soil modulus ratios

3.3 Case Study

Bridge piers constituted by single columns and founded on inclined pile groups with different configurations and different pile inclinations are investigated (Figure 13). These are representative of the transverse response of multi-span bridges with steel-concrete composite continuous deck and characterised by a span length of approx. 25 m. The pier has a solid square cross section of edge 2.00 m and its mass is consistently distributed along the column. The piers' heights is equal to 15 m, including the pile cap thickness. The concrete is of grade C30/37 and is considered to be linearly elastic with Young's modulus $E_c = 3.5 \times 10^7$ kN/m². Cracking effects are accounted for by considering an effective modulus of elasticity $E_{c,eff} = 0.75E_c$. The pier is discretized by 1 m long beam finite elements. Foundations are constituted by piles of diameter $D = 1$ m and length $L = 30$ m. The piles cap is considered to be rigid with a master node placed in correspondence of its centroid. A 5% stiffness proportional damping for the first mode is introduced in terms of Rayleigh damping. The soil profile falls within the type C of the N 1998-1-1 [9] and consists of a 40 m thick three-layered soil deposit overlying a bedrock. Mechanical properties of soils constituting the deposit are reported in Figure 13b; the shear modulus degradation and damping evolution curves suggested by Vucetic & Dobry [10] for soft clays are adopted to account for the nonlinear behaviour of the soil, in a linear equivalent manner. To assess the behaviour of the bridges a specific strategy has been adopted.

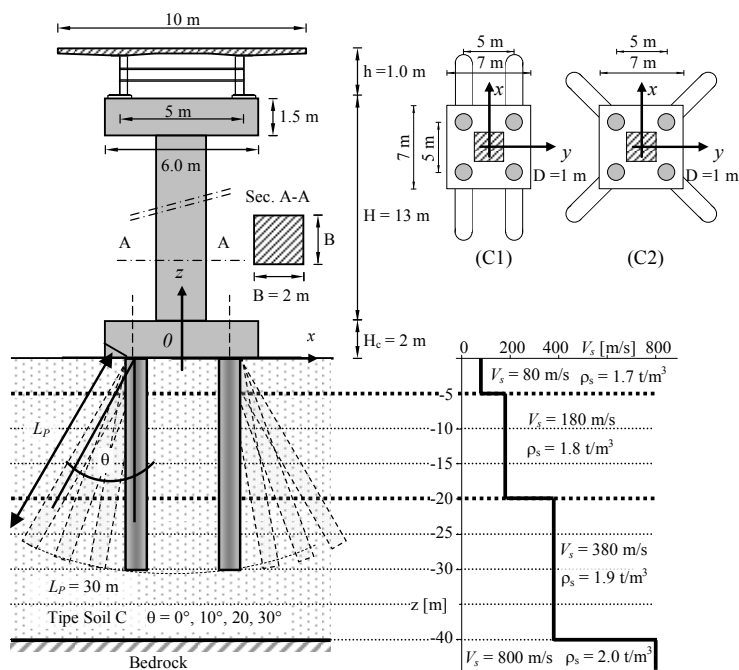


Figure 13. Case studies

Real accelerograms have been selected with reference to rock outcropping sites (soil type A), iteratively propagated by means of a 1D site response analysis and scaled to achieve at the deposit surface the design spectral acceleration at the fundamental period of the bridge (at fixed base condition). Seven ground motions, recorded on site class A, are thus selected [11] from the European Strong Motion Database (Ambraseys et al., [12]) to represent the seismic shaking at the outcropping bedrock (Figure 14). In the site response analysis the nonlinear soil behaviour is taken into account in a linear equivalent manner.

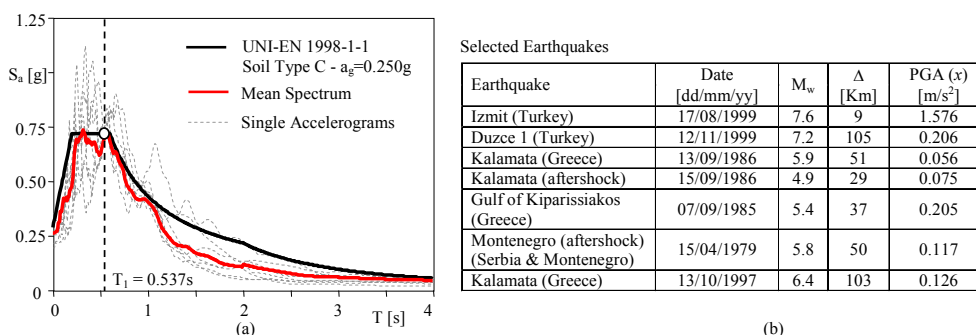


Figure 14. (a) Comparison between the mean acceleration response spectrum at the ground surface and the code spectrum; (b) acceleration response spectra of selected earthquakes

Figure 14a compares the obtained mean geometric acceleration response spectrum at the ground surface (red line) with the relevant code defined response spectrum (black line). Since the soil has a nonlinear behaviour, amplification effects depend on the earthquake frequency content and on the scale factor necessary to achieve the target spectral ordinate; major site effects are evident, for the case study, in the period range 0.25÷1 s.

Figure 15 shows mean values of the global stress resultants in one pile of the group and the mean inertial stress resultants along the bridge pier for the group configuration C1, obtained by considering different pile rake angles. The rake angle affects sensible both the pile and pier stress resultants: as for piles, by increasing the pile rake angle the axial force in proximity of the pile head decreases while increases along the pile shaft for depth greater than 5 m. Peaks of shear force and bending moment at the interfaces between different layers tend to decrease by increasing the pile rake angle. Concerning the superstructure mean shear and bending moments decrease by increasing the pile inclination.

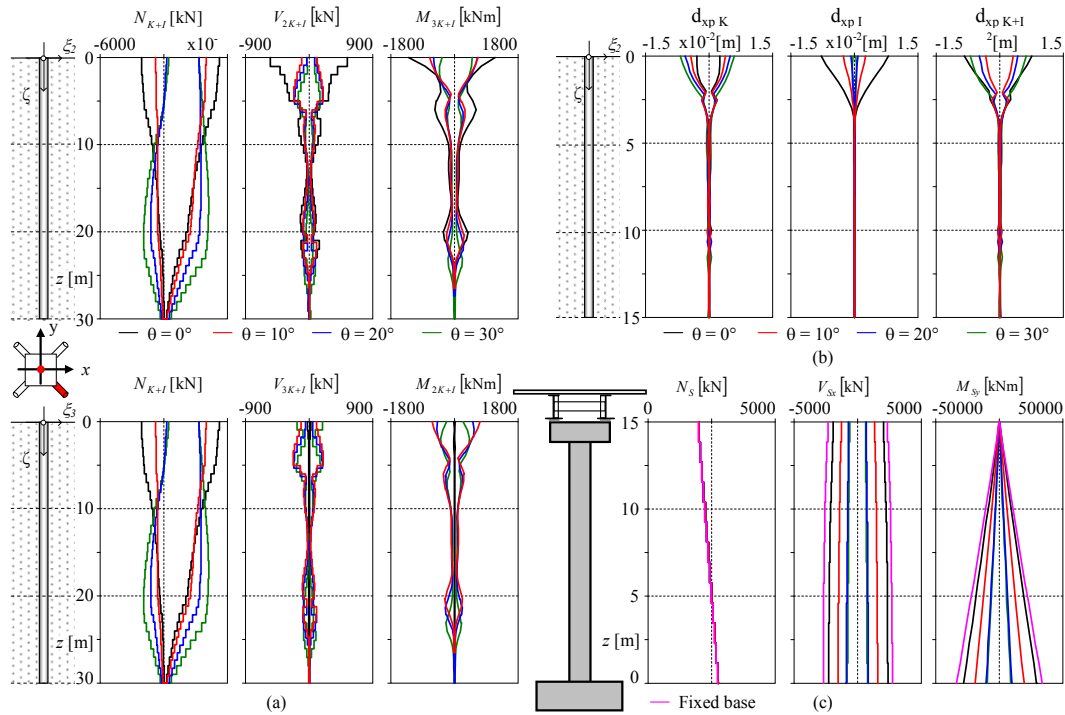


Figure 15. Results for configuration C1: (a) Global mean (K+I) stress resultants in one pile of the group; (b) Kinematic, Inertial and global soil displacement in one pile of the group; (c) Inertial stress resultants in the bridge pier.

3.4 Conclusion

A 3D numerical model for the evaluation of the dynamic impedance functions of inclined pile groups has been presented. Piles are modelled with beam finite elements and the soil is assumed to be a horizontally layered half-space. The problem is formulated in the frequency domain, under the assumption of linear behaviour for both soil and piles. The pile-soil-pile interaction as well as the radiation damping is accounted for by means of elastodynamic Green's functions. The model validation is carried out performing accuracy analyses and comparing results, in terms of dynamic impedances, kinematic response parameters and pile stress resultants, with those furnished by 3D finite element models.

The model is able to capture the vertical, rotational and coupled roto-translational response of pile foundations with inclined piles, obtained from refined and highly computational demanding 3D finite element models. Furthermore, the kinematic response of the

soil-foundation system as well the kinematic stress resultants along the piles due to propagating (seismic) shear waves is accurately predicted.

Considering that convergence of results is assured even for coarse meshes, the computational effort reduces drastically with respect to 3D solid finite element models; with reference to the performed applications, the number of dof reduces of about 2 order of magnitudes, with a significant saving of the analysis time.

The proposed model constitutes a versatile practical tool that furnishes the soil-foundation impedance functions and the foundation input motion of inclined pile groups; these may be used, in the frame of the substructure approach, to perform complete dynamic soil-structure interaction analyses of structures on such kind of foundations. Moreover, the model may be used to investigate the kinematic response of pile foundations with inclined piles (e.g. effects of the pile rake angle on pile kinematic stress resultants, soil-foundation compliance and foundation input motion) contributing to renovate the engineers confidence to the use of inclined piles.

References

- [1] EN 1998-5. *Eurocode 8: Design of structures for earthquake resistance - Part 5: Foundations, retaining structures and geotechnical aspects*, 2004.
- [2] NTC2008. *Technical rules for constructions*. (in Italian), 2008.
- [3] D. Mitchell, R. Tinawi, R.G. Sexsmith. *Performance of bridges in the 1989 Loma Prieta earthquake, Lessons for Canadian designers*. Can J Civil Eng 18(4): 711–734, 1991.
- [4] M. Sadek, I. Shahrour. *Three-dimensional finite element analysis of the seismic behaviour of inclined micropiles*. Soil Dyn Earthquake Engng 24, pp 473–485, 2004.
- [5] N. Gerolymos, A. Giannakou, I. Anastasopoulos, G. Gazetas. *Evidence of beneficial role of inclined piles: observations and summary of numerical analyses*. Bulletin of Earthquake Engineering 6(4): 705–722, 2008.
- [6] A. Giannakou, N. Gerolymos, G. Gazetas, T. Tazoh, I. Anastasopoulos. *Seismic Behavior of Batter Piles: Elastic Response*. Journal of Geotechnical and Geoenvironmental Engineering 136: 1187–1199, 2010.
- [7] L.A. Padrón, J.J. Aznárez, O. Maeso, A. Santana. *Dynamic stiffness of deep foundations with inclined piles*. Earthquake Engineering & Structural Dynamics, 39(12): 1343–1367, 2010.
- [8] F. Dezi, S. Carbonari, and G. Leoni. *A model for the 3D kinematic interaction analysis of pile groups in layered soils*. Earthquake Engineering & Structural Dynamics, 38(11), 1281–305, 2009.
- [9] EN 1998-1. *Eurocode 8: Design of structures for earthquake resistance - Part 1: General rules, seismic actions and rules for buildings*, 2005.
- [10] M. Vucetic, R. Dobry. *Effect of soil plasticity on cyclic response*. Journ. of Geot. Eng. ASCE. 117(1), 89–107, 1991.
- [11] I. Iervolino, C. Cornell. *Record selection for nonlinear seismic analysis of structures*. Earthquake Spectra 21(3), 685–713, 2005.
- [12] N. Ambraseys, P Smit, R. Sigbjornsson, P. Suhadolc, B. Margaris. *Internet-Site for European Strong-Motion Data*. Europ. Commission, Research-Directorate General, Environment and Climate Programme, 2002 (http://www.isesd.hi.is/ESD_Local/home.htm).